

## GENERAL ARTICLE

# Nurr1 repression mediates cardinal features of Parkinson's disease in $\alpha$ -synuclein transgenic mice

Maria Argyroftalmidou<sup>1</sup>, Athanasios D. Spathis<sup>1</sup>, Matina Maniati<sup>1</sup>, Amalia Poula<sup>1</sup>, Maira A. Katsianou<sup>1,†</sup>, Evangelos Sotiriou<sup>1</sup>, Maria Manousaki<sup>1</sup>, Celine Perier<sup>2</sup>, Ioanna Papapanagiotou<sup>1</sup>, Zeta Papadopoulou-Daifoti<sup>3,‡</sup>, Pothitos M. Pitychoutis<sup>3,4</sup>, Pavlos Alexakos<sup>1</sup>, Miquel Vila<sup>2</sup>, Leonidas Stefanis<sup>1,5</sup> and Demetrios K. Vassilatis<sup>1,\*</sup>

<sup>1</sup>Center for Clinical Research, Experimental Surgery and Translational Research, Biomedical Research Foundation of the Academy of Athens, Athens 11527, Greece, <sup>2</sup>Research Institute, University Hospital Vall d'Hebron, Barcelona 08035, Spain, <sup>3</sup>Department of Pharmacology, Medical School, University of Athens, Athens 11527, Greece, <sup>4</sup>Department of Biology & Center for Tissue Regeneration and Engineering at Dayton (TREND), University of Dayton, Dayton, OH 45469-2320, USA and <sup>5</sup>Second Department of Neurology, National and Kapodistrian University of Athens Medical School, Athens 11527, Greece

\*To whom correspondence should be addressed. Tel: +30 2106597456; Fax: +30 2106507545; Email: [dvassilatis@bioacademy.gr](mailto:dvassilatis@bioacademy.gr)

## Abstract

Duplication/triplication mutations of the SNCA locus, encoding alpha-synuclein (ASYN), and loss of function mutations in Nurr1, a nuclear receptor guiding midbrain dopaminergic neuron development, are associated with familial Parkinson's disease (PD). As we age, the expression levels of these two genes in midbrain dopaminergic neurons follow opposite directions and ASYN expression increases while the expression of Nurr1 decreases. We investigated the effect of ASYN and Nurr1 age-related expression alterations in the pathogenesis of PD by coupling Nurr1 hemizygous with ASYN(s) (heterozygote) or ASYN(d) (homozygote) transgenic mice. ASYN(d)/Nurr1+/- (2-hit) mice, contrary to the individual genetic traits, developed phenotypes consistent with dopaminergic dysfunction. Aging '2-hit' mice manifested kyphosis, severe rigid paralysis, L-DOPA responsive movement impairment and cachexia and died prematurely. Pathological abnormalities of phenotypic mice included SN neuron degeneration, extensive neuroinflammation and enhanced ASYN aggregation. Mice with two wt Nurr1 alleles [ASYN(d)/Nurr1+/+] or with reduced ASYN load [ASYN(s)/Nurr1+/-] did not develop the phenotype or pathology. Critically, we found that aging ASYN(d), in contrast to ASYN(s), mice suppress Nurr1-protein levels in a brain region-specific manner, which in addition to Nurr1 hemizygosity is necessary to instigate PD pathogenesis. Our experiments demonstrate that ASYN-dependent PD-related pathophysiology is mediated at least in part by Nurr1 down-regulation.

<sup>†</sup>Present address: Department of Biological Chemistry—Cellular and Molecular Biomechanics Unit, Medical School, National and Kapodistrian University of Athens, 11527 Athens, Greece.

<sup>‡</sup>Deceased.

Received: March 4, 2021. Revised: April 17, 2021. Accepted: April 19, 2021

© The Author(s) 2021. Published by Oxford University Press.

This is an Open Access article distributed under the terms of the Creative Commons Attribution Non-Commercial License (<http://creativecommons.org/licenses/by-nc/4.0/>), which permits non-commercial re-use, distribution, and reproduction in any medium, provided the original work is properly cited. For commercial re-use, please contact [journals.permissions@oup.com](mailto:journals.permissions@oup.com)

## Introduction

Parkinson's disease (PD) is characterized by the gradual degeneration of midbrain dopaminergic neurons. The consequent depletion of dopamine (DA) in the striatum results in movement abnormalities, which are the principal symptoms of the disease. DA replenishment strategies improve movement, but disease-modifying therapies have not been discovered. Both genetic and environmental factors are implicated in PD etiology, but aging is also critical as disease prevalence increases almost 400 times the crude incidence rate in people aged over 85 (1–3).

Several PD-associated mutant loci have been identified providing insight into the pathogenic mechanisms of the disease. Alpha-synuclein (ASYN), an abundant presynaptic protein and the primary structural component of Lewy bodies (4), is linked to both the etiology and the pathogenesis of PD. Mutations altering single amino acid codons (5) or increasing the copy number (6,7) of ASYN have been identified in PD patients. However, ASYN-overexpressing rodents commonly present inconsistent alterations of motor functions and little or no loss of substantia nigra (SN) dopaminergic neurons, and aberrant accumulation of insoluble proteins has been detected only in some (8).

Mutations down-regulating the expression of *Nurr1*, a nuclear receptor that directs the differentiation of committed neuronal precursors to the full dopaminergic phenotype, have been discovered in both familial and sporadic PD cases (9–13). *Nurr1* deletion in mice is lethal; nevertheless, several lines of evidence have strongly associated *Nurr1* down-regulation with PD and reduced dopaminergic neuron survival (9) *in vivo*. *Nurr1*<sup>+/-</sup> mice show changes in dopamine signaling (14–16) and enhanced susceptibility to the mitochondrial toxin MPTP (17), while reduced *Nurr1* expression in microglia results in exaggerated inflammatory response leading to dopamine neuron death (18).

Age-dependent alterations of SN ASYN and *Nurr1* expression follow the genetic trend correlating with dopaminergic neuron loss and reduced tyrosine hydroxylase (TH) transcription. Autopsy studies in humans and rhesus monkeys (19) show a robust age-related SN-specific expression increase of ASYN and diminished TH expression (20). On the contrary, SN *Nurr1* expression progressively decreases with increasing age (21,22). Experiments in cells support the opposing expression effects between ASYN and *Nurr1*. Transfection of ASYN in SH-SY5Y (23) or HEK293 (24) cells suppresses endogenous *Nurr1* levels, while viral ASYN overexpression in rat DA neurons disrupts *Nurr1*-dependent GDNF signaling (25).

As ASYN is thought of as a mediator of aging (26) while *Nurr1* is thought to counteract established aging hallmarks (27), we investigated the significance of the looming interaction between ASYN and *Nurr1* in mice approximating aged humans in terms of their relative expression. We created mice with the *Nurr1*<sup>+/-</sup> genotype complemented with different ASYN backgrounds ranging from wt to ASYN(s) +/- or ASYN(d) +/- transgenics. We show that aging ASYN(d)/*Nurr1*<sup>+/-</sup> mice, contrary to the individual genetic traits, develop cardinal phenotypic and pathological features of PD. Furthermore, we show that ASYN-dependent *Nurr1* down-regulation during aging is critical for PD pathogenesis.

## Results

### Creation and phenotypic characterization of '2-hit' mice

We outcrossed 129/SV *Nurr1*<sup>+/-</sup> mice (14) with C57BL/6 J transgenic mice expressing human A53T-ASYN under the Prion promoter (Jackson Labs, 28). Intercrossing double heterozygote F1 animals, we obtained F2 experimental animals at the expected frequencies (Fig. 1A). With the exception of *Nurr1*<sup>-/-</sup>, which died after birth, all other animals developed normally with no apparent deficits. In contrast to wt and ASYN(d), which gained weight with increasing age, the weight of *Nurr1*<sup>+/-</sup> and '2-hit' animals was relatively stable throughout their life. At 6 months of age, the weight of the animals did not differ among genotypes (data not shown). While at 9 months of age, weight differences among genotypes were noticeable, and at 12 months of age, they were evident, signifying a trend; however, still, they were not statistically significant (Fig. 1B). As the animals aged further, the weight differences of 15- and 18-month-old *Nurr1*<sup>+/-</sup> and '2-hit' animal weights were significantly lower by ~1/3 of those of wt animals (Fig. 1B). The weight of ASYN(s) and ASYN(s)/*Nurr1*<sup>+/-</sup> was not different than that of wt animals at any age (data not shown).

Locomotor activity was measured in an activity box during three consecutive days for 10 min each day. At 6 months of age, '2-hit' mice total spontaneous locomotor activity was lower by ~40% in comparison to coeval wt, *Nurr1*<sup>+/-</sup> or ASYN(s)/*Nurr1*<sup>+/-</sup> animals (Fig. 1C). Total activity was restored to normal in *Nurr1*<sup>+/+</sup> ASYN(s) and ASYN(d) animals (Fig. 1C). Surprisingly, '2-hit' animal total locomotion at 9 or 12 months was not statistically different than that of controls (Fig. 1D). Analyzing collectively the activity of all *Nurr1*<sup>+/-</sup> genotypes in comparison to the collective activity of the *Nurr1*<sup>+/+</sup> genotypes, we were able to attribute this to *Nurr1* levels. Nine-month-old mice of the *Nurr1*<sup>+/-</sup> genotype mice collectively had ~18% higher total activity than that of the *Nurr1*<sup>+/+</sup> genotypes. This difference increased to ~45% for 12-month-old mice. These measurements are similar to the activity of *Nurr1*<sup>+/-</sup> animals observed by others (29,30). We analyzed separately day 1 locomotion, which represents exploratory activity. All animals had a significant decline in exploratory activity during aging; however, this decline was less pronounced in the '2-hit' animals (Fig. 1E), a phenomenon shared with the other animals of the *Nurr1*<sup>+/-</sup> genotype. The combined *Nurr1*<sup>+/-</sup> genotypes revealed an increased exploratory activity as the animals aged in comparison to the combined *Nurr1*<sup>+/+</sup> genotypes regardless of ASYN-Tg expression showing a *Nurr1*-dependent phenotype, which affected the total activity. No differences in forced movement, coordination, balance and endurance could be detected by the rotarod test (Fig. 1F). At 15 months of age, we observed that '2-hit' mice had considerably shorter stride length (6.19 ± 0.16 cm) (Fig. 1G). The reduced stride length increased to wt levels in the *Nurr1*<sup>+/+</sup> background of coeval ASYN(d) mice (7.0 ± 0.20 cm), indicating the dependence of the compromised movement on *Nurr1* levels. We did not detect any gender differences in any of the tests described above.

### Striatal dopamine level attenuation and dopaminergic neuron loss in '2-hit' animals

Striatal dopamine (DA), homovanillic acid (HVA) and 3,4-dihydroxyphenylacetic acid (DOPAC) levels of 12- to

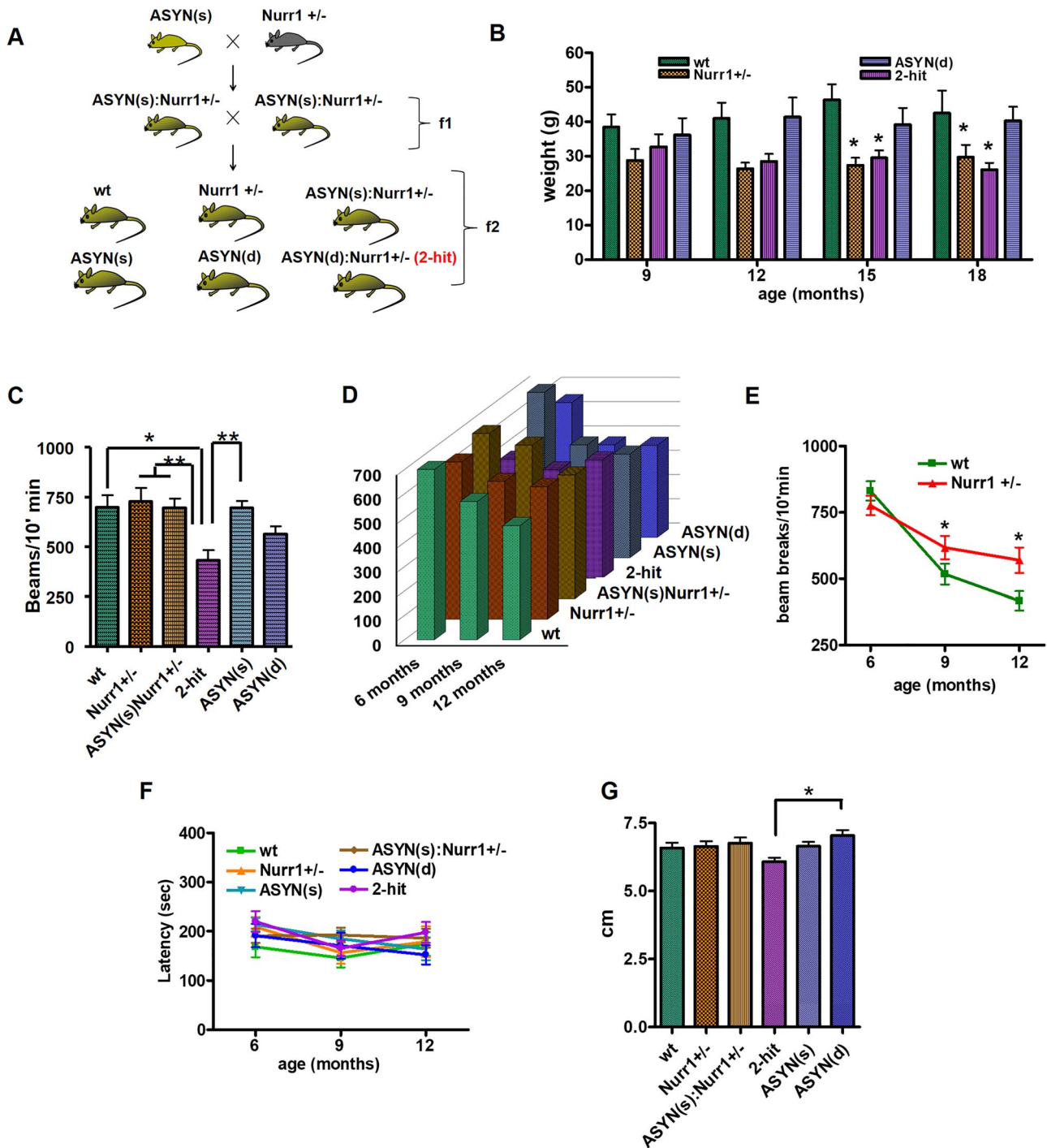


**Figure 1.** Generation and phenotypic characterization of '2-hit' mice. (A) Breeding strategy scheme. (B) The weight of Nurr1<sup>+/-</sup> and '2-hit' animals was considerably lower than wt animals becoming more apparent with increasing age (two-way ANOVA, Bonferroni's Multiple Comparison Test,  $P=0.0001$ ). Data presented as mean  $\pm$  SEM. \* $P < 0.05$ , \*\* $P < 0.01$ , \*\*\* $P < 0.001$ . (C) Total activity at the age of 6 months of '2-hit' mice is reduced in comparison to the other experimental animals (one-way ANOVA, Bonferroni's Multiple Comparison Test,  $P=0.0007$ ,  $n=23-28$ ). (D) Activity was monitored in age- and gender-matched mice at the ages of 6, 9 and 12 months. At the ages of 9 and 12 months, there are no statistically significant differences between the genotypes. (E) Day 1 exploratory activity decline during aging was less pronounced for the combined Nurr1<sup>+/-</sup> genotypes in comparison to the combined Nurr1<sup>+/+</sup> genotypes regardless of ASYN-Tg expression (two-way ANOVA, Bonferroni's Multiple Comparison Test, genotype  $P=0.044$ , age  $P < 0.0001$ , interaction  $P=0.02$ ,  $n=36-46$ ). (F) No differences in forced movement, coordination, balance and endurance could be detected between any of the genotypes as assessed by the rotarod test. (G) Stride length at 15 months of age. Shorter stride length (one-way ANOVA, Bonferroni's Multiple Comparison Test,  $P=0.03$ ,  $n=15-18$ ) of '2-hit' mice against ASYN(d) mice.

18-month-old Nurr1<sup>+/-</sup>, ASYN(s) and ASYN(s)/Nurr<sup>+/-</sup> mice were not different from those of coeval wt animals. Unlike other ASYN overexpressing lines (31,32), we found that 12- to

18-month-old ASYN(d) mice had robustly elevated DA, HVA and DOPAC levels by 29, 54 and 42%, respectively, in comparison to the other genotypes (Fig. 2A). This potent DA increase is

not uncommon in ASYN(d)A53T transgenic animals (33,34) and indicates that DA levels of '2-hit' animals, despite the apparently physiological DA values, were attenuated due to Nurr1 haploinsufficiency and could induce dopamine deficiency to the ASYN(d) genetic background.

Unbiased stereological counting of SN TH(+) neurons in 12- to 18-month-old '2-hit' mice showed ~20% fewer neurons ( $3321 \pm 179$ ,  $n=8$ ) in comparison to other genotypes (wt  $4054 \pm 128$ ,  $n=5$ ; Nurr1+/-  $3998 \pm 204$ ,  $n=9$ ; ASYN(s)/Nurr1+/-  $4200 \pm 140.0$ ,  $n=5$ ), (Fig. 2B and C) indicating a synergistic effect of the opposite Nurr1 and ASYN expression on SN TH(+) neuron loss. Notably, Nurr1+/+ ASYN(s) and ASYN(d) animal SN TH(+) neuron counts ( $4240 \pm 327$ ,  $n=5$ ;  $4301 \pm 130$ ,  $n=8$ , respectively) were essentially equal to wt levels, showing that Nurr1 hemizygoty is required for dopaminergic neuron loss (Fig. 2C).

### Nurr1 and ASYN synergy in the manifestation of a PD-like phenotype

'2-hit' mice had significantly shorter lifespan (Fig. 3A) due to the appearance of severe progressive motor phenotype in approximately 40% of the animals between 12 and 22 months of age (Fig. 3B). The initial symptoms were low body weight, hunched backs, stretched tails and asymmetrical hind limb movements when suspended by the tail. Progressively, within 1 to 8 weeks, phenotypic mice became stiff, particularly at their hind limbs and tails, and reluctant to initiate movement, a characteristic reminiscent of PD (Fig. 3C; Supplementary Material, Videos S1 and S2). Eventually, phenotypic mice were unable to reach for food or water and lost ~35% body weight during the last month of each of the animals' life (Fig. 3D); however, their survival could be prolonged by bottom-cage feeding. Final-stage animals crawled on forelimbs while the righting reflex, demonstrating agility, was particularly impaired (Supplementary Material, Video S3). Phenotypic animals had even fewer SN TH(+) neurons by 11.8% ( $2950 \pm 166$ ,  $n=5$ ) compared to age-matched non-phenotypic '2-hit' animals (although non-statistically significant). However, phenotypic animal SN TH(+) neuron counts were reduced significantly in comparison to the counts of all the animals of the other genotypes by 27%, versus wt; 25% versus Nurr1+/-; 37% versus ASYN(s):Nurr1+/-; 33% versus ASYN(s) and 32% versus ASYN(d) (Fig. 3E). Comparison of Nissl-stained SN section counts between ASYN(d) transgenics 100.0% ( $\pm 0.9$ ) and phenotypic and non-phenotypic '2-hit' animals revealed a reduction of neuron cell bodies to 86% ( $\pm 4.2$ ) and to 84% ( $\pm 13$ ) respectively, which showed the same tendency as the TH(+) stereological counts; nevertheless, it was not statistically significant. Animals in the Nurr1+/+ background, irrespective of the ASYN genetic background, had normal lifespan and normal SN TH(+) neuron counts and did not develop the PD-like phenotype up to the age of 24 months indicating the importance of Nurr1 levels in the development of cardinal features of PD in mice. Furthermore, enteric function of phenotypic mice was assessed by stool analysis. Total hourly stool weight of phenotypic mice was reduced in comparison to non-phenotypic mice (Fig. 3F) and dry hourly stool weight (Fig. 3G) was significantly lower. However, dry/water stool ratio was similar, indicating that the dramatic weight loss of phenotypic mice was due to reduced food intake (Fig. 3H).

### L-DOPA administration improved movement of phenotypic animals

The motor function of '2-hit' mice deteriorated dramatically upon phenotype appearance. Rotarod performance could not be evaluated because of the complete lack of coordination and balance. Stride length (Fig. 4A) however could be measured. L-DOPA/carbidopa (5 mg/kg and 0.5 mg/kg, respectively) IP injections improved the stride length of phenotypic mice, L1, ( $3.8 \pm 0.33$  versus  $2.4 \pm 0.06$  cm); H1 ( $3.0 \pm 0.3$  versus  $2.1 \pm 0.18$  cm); and G8, ( $5.2 \pm 0.12$  versus  $4.05 \pm 0.17$  cm) over baseline stride length, which was determined the previous day (Fig. 4B). On the contrary, repeating the same experiment for each phenotypic mouse with saline injections had no effect. L-DOPA administration improved stride length, on average, by 43.3% (Fig. 4C; Supplementary Material, Videos S4 and S5). The L-DOPA response could be detected as early as 20 min after administration and lasted for up to 60 min (Fig. 4D). L-DOPA/carbidopa injections did not have any effect on the stride length of coeval non-phenotypic animals (Fig. 4E) indicating that the dopaminergic deficits are directly implicated in the phenotype.

### '2-hit' phenotypic mice show increased neuroinflammation

Neuroinflammation was initially assessed by staining with the microglia activation marker CD45 (Fig. 5A-C). Relative staining was quantitated and it was found that between non-phenotypic and phenotypic mice it was increased ~200% in the latter (Fig. 5D). The microglia of phenotypic mice appeared activated having enlarged, swollen cell bodies and truncated processes (Fig. 5A and B). Remarkably, Nurr1+/- and ASYN(s):Nurr1+/- mice showed no microglia activation, signifying the requirement of neuronal ASYN overexpression. Additionally, comparison between non-phenotypic '2 hit' and ASYN(d):Nurr1+/+ mouse midbrain CD45 staining (Fig. 5A and C) was decreased by almost 10-fold (Fig. 5E) demonstrating that maintenance of Nurr1 expression indeed protects mice from exaggerated neuroinflammation (18). IBA1 staining of phenotypic mice midbrain sections and comparison with non-phenotypic '2-hit' animals corroborated the above results revealing activated microglia with the characteristic morphology (Fig. 5F and G). Furthermore, we assessed galectin-3 (Gal-3) expression, which is triggered upon neuroinflammation and has been shown to modulate the expression of pro-inflammatory factors, such as iNOS, TNF- $\alpha$  and IL-1 $\beta$ , in microglia (35,36). Immunofluorescence staining of midbrain sections revealed limited Gal-3 expression in non-phenotypic '2-hit' animals (Fig. 5H). However, in phenotypic mice, microglia Gal-3 expression was widespread and the number of Gal-3-positive cells was considerably increased (Fig. 5I). These results provide compelling evidence that ASYN overexpression and Nurr1 down-regulation result in the manifestation of neuroinflammation in '2-hit' mice.

### '2-hit' phenotypic mice show ASYN aggregation

Midbrain dopaminergic neurons of 12- to 18-month-old mice revealed robust ASYN immunostaining in both non-phenotypic (Fig. 6A) and phenotypic (Fig. 6B) animals, the latter appearing more intense. Dopaminergic neuron ASYN immunostaining of coeval ASYN(d):Nurr1+/+ (Fig. 6C) was weaker suggesting that Nurr1 haploinsufficiency affects ASYN accumulation. We also

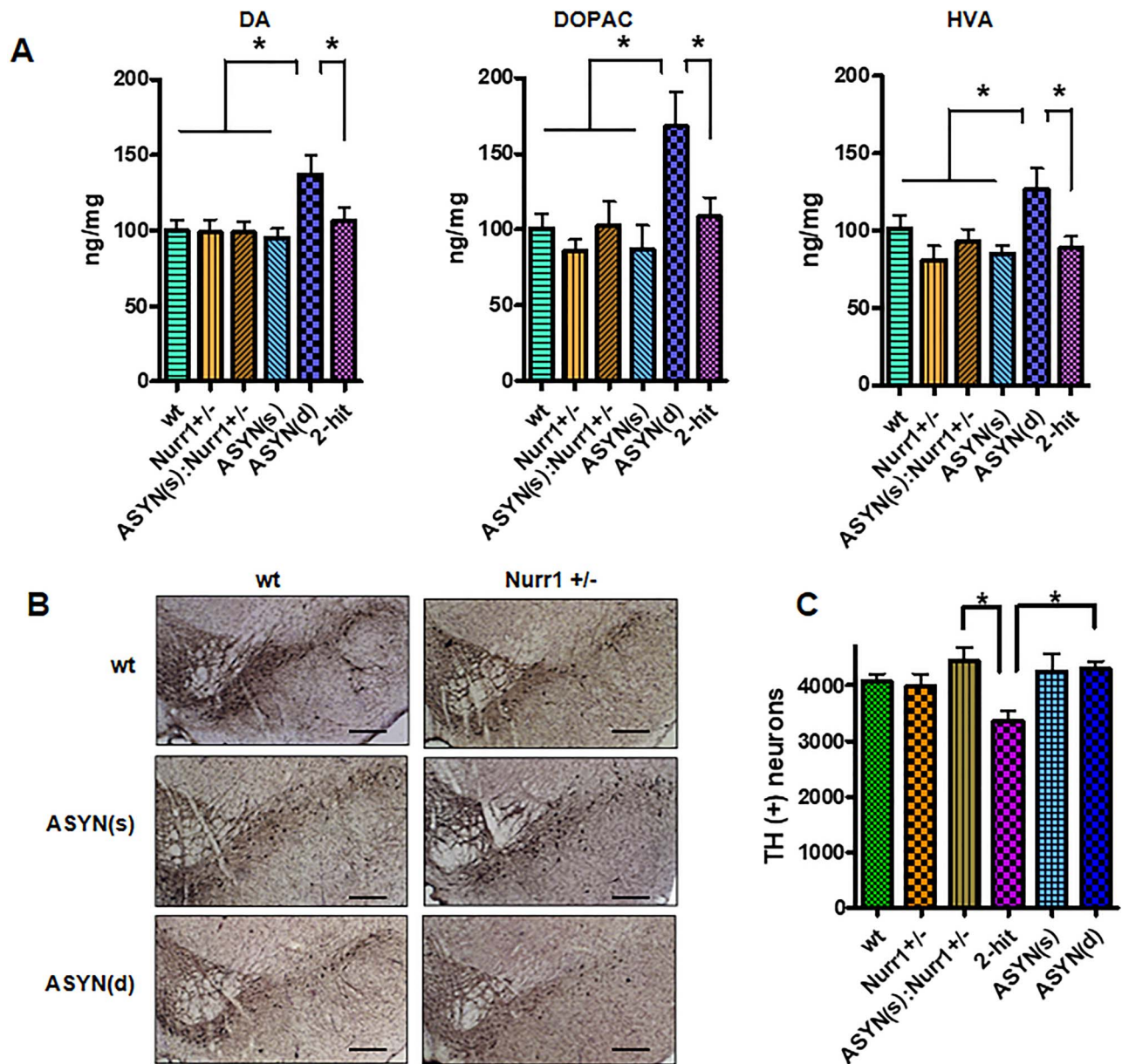


**Figure 2.** Dopaminergic evaluation of '2-hit' mice. (A) DA, DOPAC and HVA levels of '2-hit' animals are attenuated relative to ASYN(d) mice due to Nurr1 haploinsufficiency (one-way ANOVA, Bonferroni's Multiple Comparison Test,  $P=0.003$ ,  $n=4-6$ ). (B) Representative photographs of SN TH immunohistochemistry of all genotypes. (C) Stereological counting of SN TH (+) neuron bodies. Each hemisphere was counted individually and the average TH (+) neuron of each animal is presented. '2-hit' animals show a statistically significant reduction of SN TH (+) neuron bodies (one-way ANOVA, Bonferroni's Multiple Comparison Test,  $P=0.4581$ ,  $n=5-11$ ) against other experimental animals. All animals were 12–18 months old.

examined for ASYN aggregation. Published results indicate that the ASYN transgenics used in our experiments overexpress highest levels of transgene in the spinal cord (28). Pilot experiments of midbrain, cortex and spinal cord protein extracts of our experimental cohorts indicated robust ASYN aggregation in the spinal cord. In order to maximize the chance of detecting ASYN aggregation in our experimental cohort, which includes Nurr1<sup>+/-</sup> animals, we quantitated the relative levels of ASYN in protein extracts in the spinal cord and the cortex by western blots. We show that homozygous ASYN transgenics overexpress ASYN 4.4 ( $\pm 0.5$ )-fold higher in comparison to non-transgenic mice ( $1 \pm 0.3$ ). Similar western blot quantification in cortex protein extracts indicated that ASYN(d) animals overexpresses ASYN only 1.2 ( $\pm 0.07$ ) times over non-transgenic animals 1.0

( $\pm 0.22$ ). The data indicate that ASYN transgene expression varies between different brain regions. Additionally, these experiments show that ASYN expression is not statistically different between ASYN(d), '2-hit' and '2-hit' phenotypic animals, suggesting that Nurr1 heterozygosity does not affect ASYN transgene expression (Fig. 6D and E). Thus, we selected to focus the investigation of ASYN aggregation on the spinal cord. Sequential spinal cord protein extraction with increasing strength detergents differentiating between soluble (Triton-X) (Fig. 6F) and insoluble (SDS) (Fig. 6G) ASYN revealed the formation of soluble and insoluble ASYN oligomers in phenotypic '2-hit' mice, the latter being particularly robust. Insoluble ASYN oligomers were essentially absent in extracts from ASYN(s) or ASYN(d) Nurr1<sup>+/+</sup> animals, as determined by western blots, suggesting

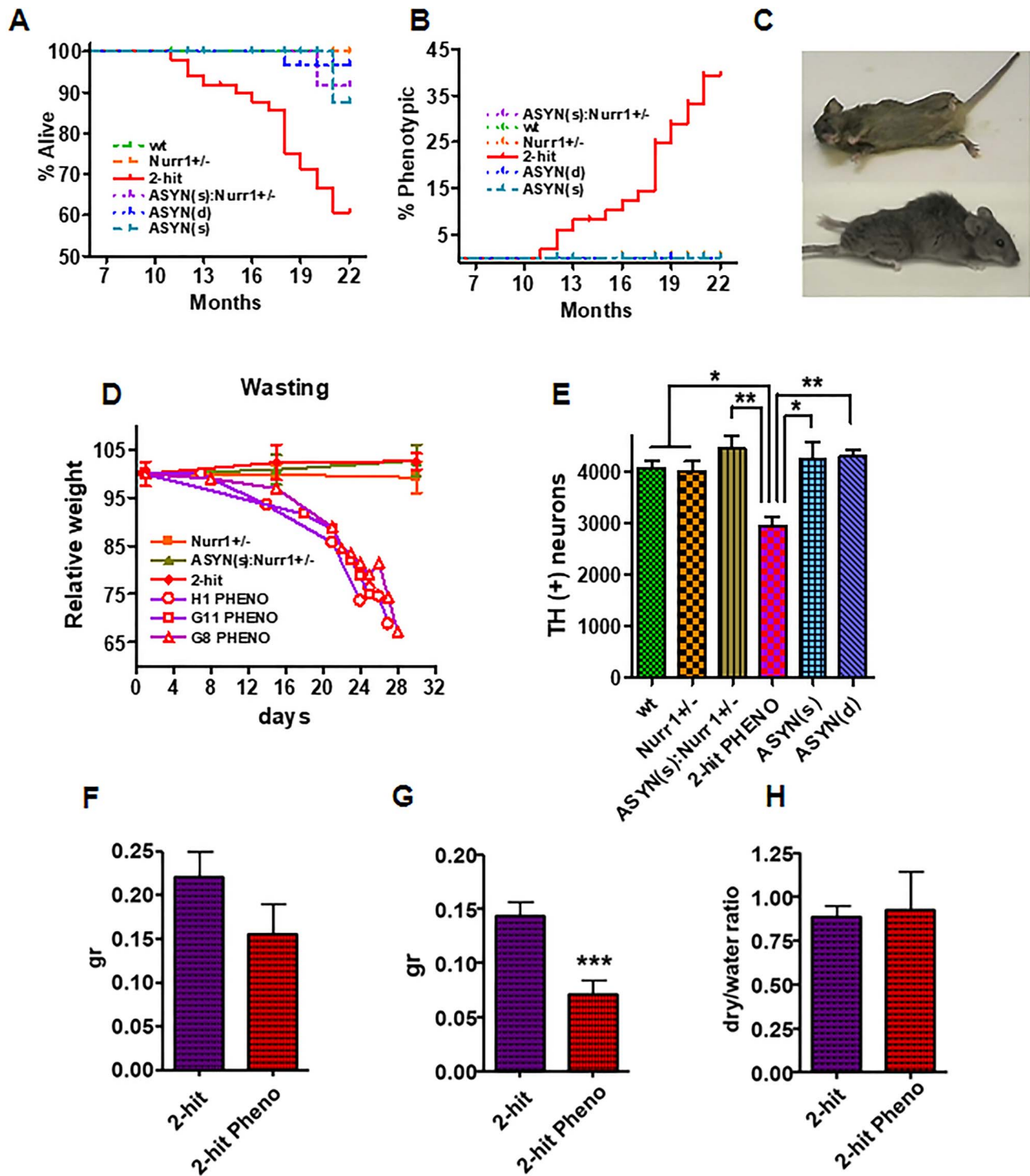


**Figure 3.** Manifestation of Parkinson's disease phenotype. (A) Survival curve for '2-hit' mice (red line) in comparison to all other genotypes ( $n=9-23$ , Logrank Test  $P < 0.0001$ ). (B) Appearance of the Parkinson's disease-like phenotype in '2-hit' mice (red line) in comparison to the other experimental animals ( $n=9-23$ , Logrank Test  $P < 0.0001$ ). (C) Representative photographs of the '2-hit' phenotype. All animals were 12–18 months old. (D) Body weight of three phenotypic '2-hit' animals during their final month as well as coeval *Nurr1*<sup>+/-</sup>, *ASYN*(s)/*Nurr1*<sup>+/-</sup> and non-phenotypic 2-hit animals. The phenotypic '2-hit' animals suffer ~35% body mass loss. (E) Reduced SN TH (+) neuron bodies of phenotypic '2-hit' mice in comparison to the other genotypes (one-way ANOVA, Bonferroni's Multiple Comparison Test,  $P = 0.003$ ,  $n = 5-11$ ). (F–H) Enteric function of phenotypic mice was normal as assessed by (F) total hourly stool weight, (G) dry hourly stool weight that was significantly lower for phenotypic mice ( $t$ -test  $P = 0.0008$ ,  $n = 6-9$ ) and (H) dry/water stool ratio that was not significantly different in comparison to non-phenotypic animals.

that *Nurr1* underexpression is a significant contributor ( $P < 0.01$ ) to *ASYN* aggregation and oligomerization. Similar western blot analysis of cortex protein extractions showed much

reduced *ASYN* oligomer formation (data not shown), which was attributed to the lower *ASYN* transgene expression in the cortex.

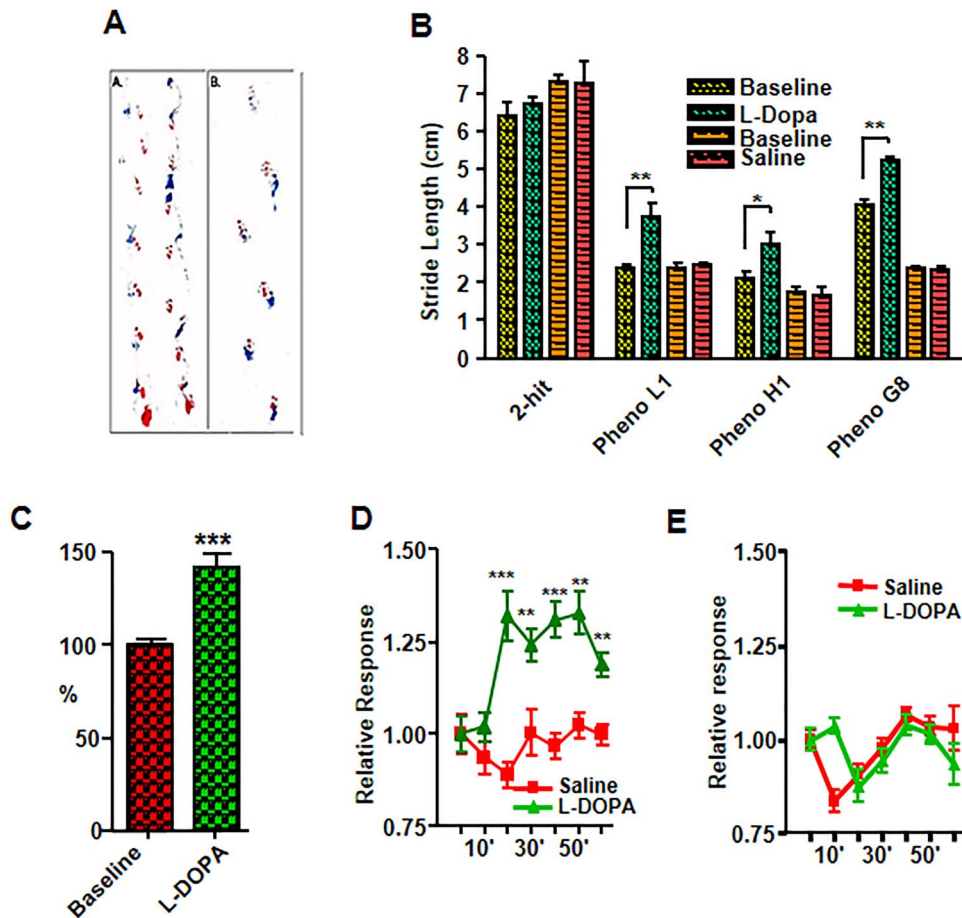


**Figure 4.** Response to L-DOPA. (A) Representative photograph of footprints from a phenotypic 18-month-old '2-hit' mouse in comparison to a non-phenotypic '2-hit' age-matched control. (B) L-DOPA administration to phenotypic '2-hit' L1, H1 and G8 and age-matched control animals. L-DOPA efficacy was measured by stride length analysis. (C) Average stride length improvement of phenotypic '2-hit' animals after L-DOPA administration was 43.3% (Student's *t*-test,  $P = 0.00002$ ,  $n = 3-5$ ). (D and E) Duration of stride length improvement of phenotypic '2-hit' animals (D) and controls (two-way ANOVA, Bonferroni's Multiple Comparison Test,  $P = 0.0001$ , treatment  $P < 0.0001$ , time  $P = 0.003$ ) (E) after L-DOPA administration (two-way ANOVA, Bonferroni's Multiple Comparison Test,  $P = 0.0001$ ). Data are presented as mean  $\pm$  SEM ( $n = 5-13$ ). \* $P < 0.05$ , \*\* $P < 0.01$ , \*\*\* $P < 0.001$ .

### Investigation of mechanisms triggering the PD-like phenotype

The genetic experiments clearly demonstrated that ASYN and Nurr1 expression levels were critical for the phenotype and pathology of '2-hit' mice. '2-hit' [ASYN(d)/Nurr1+/-] mice manifested cardinal features of PD, while normozygous Nurr1 (ASYN(d)/Nurr1+/+) or ASYN(s)/Nurr1+/- animals did not develop PD-like symptoms or pathology. These experiments indicated that the combination of ASYN overexpression and Nurr1 down-regulation are essential and sufficient to cause PD-related abnormalities. Nevertheless, how the higher ASYN expression instigates the PD-like phenotype and pathology was obscure.

We investigated for possible ASYN copy number variations within the same ASYN genotype by genomic DNA qPCR; however, the results were unvaried (data not shown), indicating that there are no transgene abnormalities.

### Progressive Nurr1 down-regulation in ASYN transgenic mice

Next, we examined Nurr1 levels in ASYN-Tg animals during aging. Various CNS regions of 4-month-old and 14-month-old

ASYN-Tg(d) and ASYN-Tg(s) mice and of coeval non-transgenic controls were analyzed by western immunoblotting (Fig. 7A-E). We did not detect any alteration in Nurr1 protein levels in the olfactory bulb, the midbrain or the spinal cord between 4-month-old ASYN-Tg(d) and wt mice (Fig. 7A-C). Nurr1 protein levels were decreased in the olfactory bulb (57%), the midbrain (35%) and in the spinal cord (65%) of 14-month-old ASYN-Tg(d) mice (Fig. 7D) in comparison to coeval non-transgenic control animals (Fig. 7D and E). Similarly, age-dependent TH protein level down-regulation has been documented in the olfactory bulb and the spinal cord of 14-month-old ASYN-Tg(d) mice (37). Interestingly, Nurr1 was not reduced in the striatum, the cortex or the cerebellum of the same animals (Fig. 7D and E). Importantly, Nurr1 is not down-regulated in olfactory bulb, midbrain and spinal cord extracts of 4- and 14-month-old ASYN-Tg(s) mice as detected by immunoblotting extending published results (37) and emphasizing the critical significance of ASYN levels. Nurr1 down-regulation in 14-month-old mice was confirmed and extended by immunohistochemical experiments in brains of 4- and 15-month-old ASYN-Tg(d) mice, where Nurr1 immunostaining was decreased in the older animal SN, but not the VTA or the cortex (Fig. 7F-H), indicating that *in vivo* increased expression of ASYN leads to an age-dependent repression of Nurr1 protein levels, as observed in aging humans (21). Finally, we did not detect Nurr1

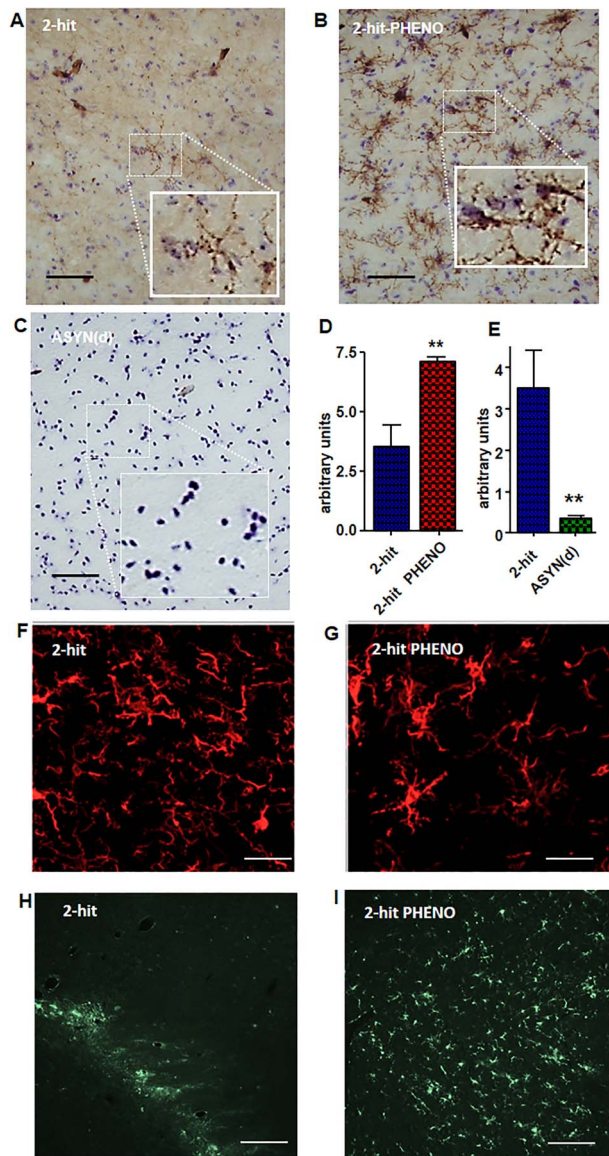


**Figure 5.** Increased neuroinflammation in '2-hit' phenotypic mice. (A–C) Immunohistochemistry of CD45 in nigral sections of 12- to 18-month-old '2-hit' non-phenotypic (A), '2-hit' phenotypic animals (B) showing increased microglia activation and ASYN-Tg(d):Nurr1+/+ animals (C) showing the weakest microglia activation. Scale bars 50  $\mu$ m. (D) Quantitation of CD45 immunoreactivity between non-phenotypic and phenotypic '2-hit' animals and ( $n=3$ ,  $t$ -test  $P=0.003$ ) (E) between non-phenotypic and ASYN-Tg(d):Nurr1+/+ animals ( $n=3$ ,  $t$ -test  $P=0.004$ ). Data are presented as mean  $\pm$  SEM ( $n=5-9$ ). \*\* $P < 0.01$ . (F and G) Microglia marker IBA1 immunofluorescence staining of midbrain sections from non-phenotypic (F) and phenotypic mice (G) (scale bar 40  $\mu$ m). (H and I) Midbrain section immunofluorescence of non-phenotypic (H) and phenotypic mice (I) staining with the anti-galectin-3 antibodies (scale bar 100  $\mu$ m).

down-regulation due to aging when we compared its protein levels in midbrain and olfactory bulb extracts between 4- and 14-month-old non-transgenic mice by immunoblotting (Fig. 7I), indicating differential Nurr1 regulation of expression between humans and mice.

#### Further Nurr1 reduction in '2-hit' mice

The relative Nurr1 expression levels in corresponding SN sections of wt, Nurr1+/- and '2-hit' mice was analyzed by

immunofluorescence. Eighteen-month-old wt mouse SN Nurr1 immunofluorescence intensity/cell (Fig. 8A) was, as expected, double that of Nurr1+/- coeval animals (49%) (Fig. 8B). SN Nurr1 expression in '2-hit' animals (Fig. 8C) was even lower by 30% versus Nurr1+/- animals and 65% versus wt animals reflecting the ASYN overexpression-dependent Nurr1 down-regulation (Fig. 8D) providing a direct link of Nurr1 levels and the '2-hit' PD-like pathology and phenotype.

## Discussion

Genetics and changes induced during aging are the paramount factors influencing PD pathogenesis (1–3,38,39). We have explored the effects of expression-level alterations induced by aging on genes in which mutations have been identified in PD patients: gain-of-function in ASYN (5) and loss-of-function mutations in Nurr1 (9). Following the same trend with the genetic data, ASYN and Nurr1 levels increase and decrease, respectively, during aging. We studied these age-related expression alterations in PD pathogenesis by generating '2-hit' mice overexpressing ASYN coupled with Nurr1 haploinsufficiency to emulate aged humans (19,21). By analyzing the whole spectrum of resulting genotypes from intercrossing Nurr1 heterozygotes and ASYN(Tg), we were able to link phenotypes with the genetic makeup of the experimental animals. In this experimental setup, neither Nurr1 heterozygotes nor ASYN(Tg) showed phenotypes significantly different than wt animals. In contrast, the phenotype of '2-hit' [ASYN(d)/Nurr1+/-] mice was consistent with mild dopaminergic deficit (Figs 1 and 2). Aging of '2-hit' mice unveiled progressive L-DOPA-responsive phenotypes evocative with later stages of PD. Phenotypic and pathological analyses showed that restoration of either genetic trait [Nurr1+/+ in ASYN(d)/Nurr1+/+ animals or ASYN(s) in ASYN(s)/Nurr1+/- animals] prevented the development of both phenotype and pathology. The genetic data indicated functional association between Nurr1 and ASYN as two subthreshold insults together in the compound '2-hit' model produce an above threshold response.

Attenuation of striatal dopamine levels (Fig. 2) of '2-hit' mice could be ascribed primarily to SN neuron loss. However, as Nurr1 regulates dopamine biosynthesis gene expression (40,41), the dopaminergic dysfunction and phenotype may also be ascribed to the inability of '2-hit' animals to sustain the compensatory activation of the dopaminergic system in the face of drastically reduced Nurr1 levels. Comparable breakdown of compensatory mechanisms has been linked to the generation of motor symptoms in human PD (42).

Approximately 40% of the '2-hit' animals up until the age of 22 months developed the PD-like phenotype. The reduced penetrance may be explained by possible variation in Nurr1 down-regulation levels in individual animals and/or, as it has been demonstrated in MPTP or genetic PD models, mouse strain-dependent genetic variations (43–45). Considering that all animals in our experiments are of mixed genetic background (50% of each 129/SV and C57BL/6 J), neither of the above possibilities can be excluded.

The genetic experiments provided strong evidence that Nurr1 down-regulation is critical for PD pathogenesis and indicated the presence of a discerning difference between the ASYN(s) and the ASYN(d) animals. We explored whether Nurr1 brain expression during aging was decisive for the phenotypic and pathological presentation of '2-hit' animals. This was indeed a critical experiment because, opposed to humans, mouse ASYN

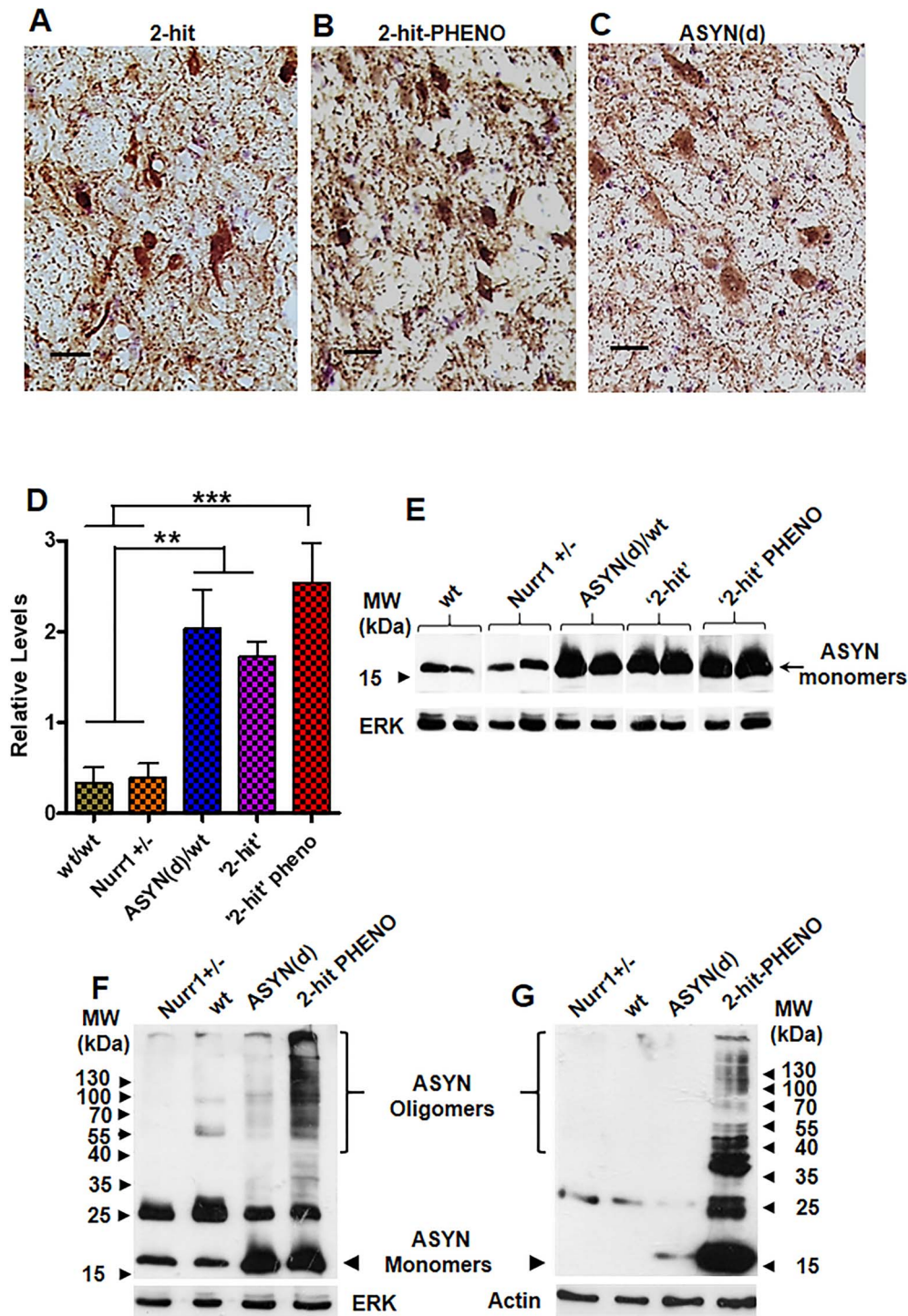


**Figure 6.** ASYN aggregation in '2-hit' phenotypic mice. (A) Representative photographs of substantia nigra ASYN immunohistochemistry of 12- to 18-month-old '2-hit' non-phenotypic (B) '2-hit' phenotypic, showing stronger intensity, and (C) ASYN-Tg(d) Nurr1<sup>+/+</sup> animals showing the weakest intensity. Scale bars 40  $\mu$ m. (D) Western blot analysis quantitation of soluble monomeric ASYN protein levels in the spinal cord after either Triton X-100 fractionation. The levels of actin in each sample were used as a loading standard. Measurements indicate that there is no statistical difference in ASYN expression between ASYN(d), '2-hit' and '2-hit' phenotypic animals. Additionally, each ASYN transgenic allele overexpresses ASYN approximately 2.9 times over non-transgenic animals (one-way ANOVA, Bonferroni's Multiple Comparison Test,  $P=0.0001$ ,  $n=4-8$ ). (E) Examples of Western blots used in the quantitation. (F) Western blot analysis of ASYN protein levels in the spinal cord after either Triton X-100 or (G) SDS fractionation. Enhanced accumulation of ASYN insoluble oligomers is detected in '2-hit' phenotypic mice in comparison to controls (association between genotype and ASYN oligomer formation, Fisher's exact test = 0.009,  $n=2-4$ /genotype). Antibodies against actin were used as a loading control. The position and size (kDa) of molecular weight markers are indicated by arrowheads.

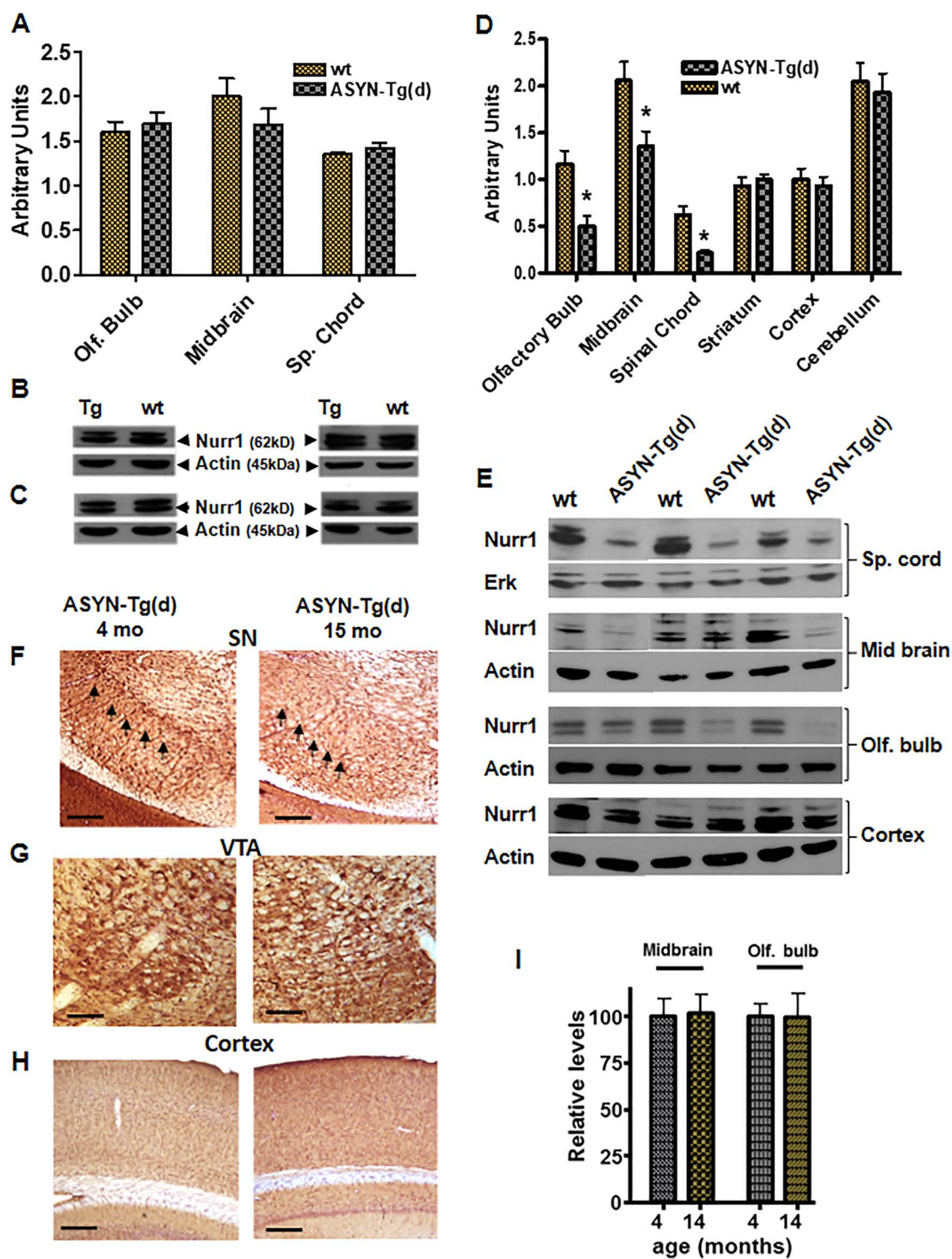


**Figure 7.** Progressive Nurr1 down-regulation in ASYN transgenic mice. (A) Western blot analysis quantitation of Nurr1 protein levels in the spinal cord, midbrain and olfactory bulb, of 4-month-old ASYN-Tg(d)/Nurr1<sup>+/+</sup> mice ( $n=5$ ), and age-matched non-transgenic mice ( $n=5$ ). (B) Representative olfactory bulb and (C) Spinal cord immunoblot images. No differences were discerned. (D) Quantitative data of Nurr1 protein levels (spinal cord, cerebellum, midbrain, olfactory bulb, striatum and cortex) of 14-month-old ASYN-Tg mice ( $n=5$ ), as well as age-matched non-Tg mice ( $n=4$ ). (E) Illustrative Nurr1 immunoblot images (spinal cord, midbrain and olfactory bulb). 14-month-old Tg mice Nurr1 protein levels were decreased in olfactory bulb, midbrain and spinal cord by 57% (t-test,  $P=0.0229$ ), 35% (t-test,  $P=0.0494$ ) and 65%, (t-test,  $P=0.0146$ ), respectively. Extracts from Nurr1 knockouts (KOs) were used as negative controls. (F–H) Nurr1 immunohistochemistry of 14-month-old control and ASYN-Tg animals. Decrease of Nurr1 immunostaining in the SN (F) (Scale bars 200  $\mu\text{m}$ ) of experimental animals but not the VTA (G) (Scale bars 100  $\mu\text{m}$ ) or the cortex (H) (Scale bars 200  $\mu\text{m}$ ). Arrows denote Nurr1 staining in the SN. (I) Comparison of midbrain and olfactory bulb Nurr1 protein levels in 4- and 14-month-old wt mice showing no variation due to aging. Data are presented as mean  $\pm$  SEM. \* $P < 0.05$ .

mRNA and protein levels are high in young mice and progressively decline in middle-aged and old mice (46). We discovered that age-dependent, brain region-specific Nurr1 protein down-regulation similar to aging humans indeed occurs in ASYN(d) mice, but not in coeval ASYN(s) or wt animals (Fig. 7) (37). Moreover, we demonstrated that Nurr1 expression per cell is further reduced in aged '2-hit' animals to approximately 35% of wt (Fig. 8). The fact that we did not detect age-dependent Nurr1 down-regulation in ASYN(s) animals suggests that the 50% reduction of Nurr1 expression due to Nurr1 hemizyosity in ASYN(s)/Nurr1+/- animals is not sufficient to instigate a behavioral phenotype or dopaminergic dysfunction. Apparently, Nurr1 down-regulation below a critical threshold (~35% of wt) is required to instigate cardinal features of PD in mice. Interestingly, the Nurr1 expression level in PD patients bearing autosomal dominant Nurr1 mutations is reduced to ~35% in comparison to healthy age-matched controls (9,13).

The observed phenotype was associated with a dramatic increase of ASYN oligomeric forms and increased neuroinflammation. Indeed, secreted ASYN has been shown to activate microglia via Toll-like receptor 2 and induce the expression of pro-inflammatory cytokines such as TNF $\alpha$  and IL-1 $\beta$  (47) whose expression is controlled by NF $\kappa$ B. Nurr1, in turn, directly binds to NF $\kappa$ B on target inflammatory gene promoters resulting in its transcriptional repression (18), while Nurr1 down-regulation in glia leads to exaggerated inflammatory responses and the production of factors that cause the loss of dopaminergic neurons (18). Furthermore, as we have shown (Fig. 5H and I) '2-hit' phenotypic mice have increased Gal-3 expression. This provides a further functional link between Nurr1 and ASYN in microglia because Gal-3 inhibition or down-regulation has been shown to affect the expression of iNOS, IL-1 $\beta$  and TNF- $\alpha$ , molecules involved in the NF $\kappa$ B pathway (35,36,47). Thus, it is reasonable to expect that ASYN overexpression combined with Nurr1 heterozygosity leads to exaggerated neuroinflammation.

An important concern of the above experiments is the possibility that the age-dependent, brain region-specific Nurr1 protein down-regulation is an effect of the genomic locus where the ASYN transgene is inserted as it is observed only in homozygote transgenic [ASYN-Tg(d)] animals. However, two different ASYN-Tg mouse lines of the same transgene were virtually identical to each other in terms of ASYN expression, ASYN aggregation and pathology indicating that the phenotypes are independent of the insertion locus (28). Furthermore, ASYN-dependent Nurr1 down-regulation in cell lines has been demonstrated by the transient overexpression of either the A53T or the wt ASYN cDNA in dopaminergic cells (23 and our unpublished experiments) or in HEK293 cells (24) or by overexpressing wt-ASYN in rat DA neurons using viral vectors. These published findings indicate that Nurr1 down-regulation is not only independent of the locus of transgene insertion but that it is also independent of the A53T mutation and that it is a function of the ASYN protein itself. Thus, additionally, we would speculate, the phenotype and the pathology of the '2-hit' mice presented in this article could also be observed in mice pan-neuronally overexpressing wt ASYN in the Nurr1 hemizygous background.

ASYN and Nurr1 have opposing functions in relation to PD pathology. Besides the ASYN-dependent Nurr1 protein level suppression, Nurr1 appears to have a reciprocal function upon ASYN as it has been shown to suppress ASYN transcription (48). As Nurr1 and ASYN repress each other, albeit by different mechanisms, dysregulation of the expression of either gene can induce a 'vicious circle' leading to the breakdown of dopaminergic neuron function and survival capable of leading to PD. It will be

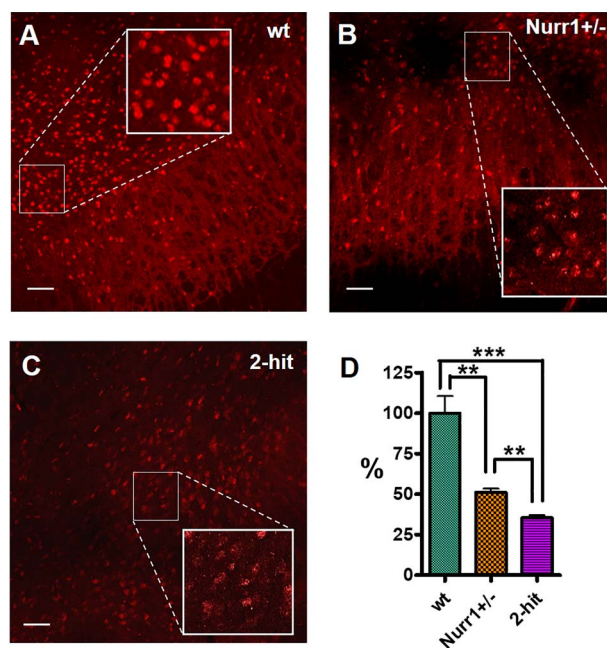


**Figure 8.** Nurr1 in '2-hit' mice. (A–C) Nurr1 immunofluorescence in the SN of Nurr1+/+, Nurr1+/- and '2-hit' animals, respectively, showing decreased Nurr1 intensity in '2-hit' animals. Scale bars 40  $\mu$ m. (D) Mean cell immunofluorescence quantitation showed that '2-hit' animals expression was decreased by 38% in comparison to Nurr1+/- (one-way ANOVA, Bonferroni's Multiple Comparison Test,  $P=0.0008$ ,  $n=3-4$ ). Data are presented as mean  $\pm$  SEM ( $n=5-9$ ). \* $P < 0.05$ , \*\* $P < 0.01$ , \*\*\* $P < 0.001$ .

particularly important to unravel the mechanisms through which ASYN leads to Nurr1 repression. Interestingly, it was recently shown that in N2a mouse neuroblastoma cells, ASYN negatively regulates Nurr1 through an NF- $\kappa$ B-related mechanism (49).

On the other hand, either lowering the expression of ASYN or inducing the expression, or the function of Nurr1 could disrupt this 'vicious circle' and can lead to a therapeutic intervention for PD. This is supported by small molecule agonists, which bind either to the ligand-binding domain of Nurr1 (50) or that of its heterodimerization partner RXR $\alpha$  (41), increase Nurr1 transcriptional activity, reduce neuroinflammation and offer disease-modifying effects in preclinical mouse PD models. Furthermore, the neuroprotection observed of Nurr1 activators in mice where dopaminergic neuron loss is induced by ASYN overexpression (41) corroborate the involvement of Nurr1 underexpression to ASYN aggregation and oligomerization (Fig. 6).

In conclusion, we show that the relative expression of two genes associated with PD, ASYN and Nurr1 during aging is critical for the development of PD pathology and phenotype in mice. Our '2-hit' model that combines genetics with aging recapitulates cardinal features of PD and in which therapeutic and mechanisms of pathogenesis could be examined. Our data support a genetic interaction between Nurr1 and ASYN and point to Nurr1 as a regulator of ASYN-mediated toxicity.

## Materials and Methods

### Animals

The Nurr1+/- (chromosome 2: 57 106 830–57 124 003 reverse strand) and the A53T ASYN Tg (chromosome 12: 48 212 716–48 212 717) mice used in this study have been described

previously (14,28). *Nurr1*<sup>+/-</sup> mice were provided by Dr Tomas Perlmann and A53T ASYN Tg mice were obtained from Jackson Laboratories. *Nurr1*<sup>+/-</sup> (129/SV) and A53T Tg<sup>+/-</sup> (C57BL/6 J) mice were crossed to obtain F1 generation (ASYN-Tg<sup>+/-</sup>:*Nurr1*<sup>+/-</sup>). F1 mice were intercrossed to obtain the six experimental genotypes in generation of F2: ASYN-Tg(-/-):*Nurr1*<sup>+/+</sup> (wt/wt), ASYN-Tg(-/-):*Nurr1*<sup>+/-</sup> (*Nurr1*<sup>+/-</sup>), ASYN-Tg(+/-):*Nurr1*<sup>+/+</sup> [ASYN(s)], ASYN-Tg(+/-):*Nurr1*<sup>+/-</sup> [ASYN(s):*Nurr1*<sup>+/-</sup>], ASYN-Tg (+/+):*Nurr1*<sup>+/+</sup> [ASYN(d)], ASYN-Tg(+/+):*Nurr1*<sup>+/-</sup> [ASYN(d)*Nurr1*<sup>+/-</sup>], '2-hit'). The lethal *Nurr1*<sup>-/-</sup> genotypes occurred at 25% frequency, while the rest of the experimental genotypes occurred at 12.5% frequency each. To minimize strain effects, all crosses were performed in a manner that genetic contribution remained 50% for each strain.

Animals were housed at the Animal Care Facilities of the Academy of Athens (BRFAA) in a pathogen-free room with controlled light-dark cycle (12 h light-12 h dark) and free access to food and water. Animal breeding and handling were performed according to the European Communities Council Directive (86/609/EEC), and ARRIVE guidelines. All animal procedures were approved by the Institutional Animal Care and Use Committee of BRFAA.

### Genotyping

Genotyping was performed by PCR on mouse tail DNA. Homozygous ASYN Tg animals were identified by quantitative Southern blot analysis with a P<sup>32</sup>-labeled oligonucleotide-primed ASYN DNA probe and verified by backcrossing, as described (14,28).

### Behavioral experiments

Behavioral experiments: all behavioral experiments were performed with age- and gender-matched controls, during the light phase, at the same time of each day.

Spontaneous locomotor activity was measured in an activity box (TSI LETICA scientific instruments) with photobeams for three consecutive days. Each animal was placed in the activity box and allowed to move freely for a period of 10 min, and beam brakes were automatically recorded.

Motor coordination and balance were tested using a Rotarod treadmill (Ugo Basile, Comerio, Italy), set to accelerating revolutions (4–40 rpm over 5 min). Each mouse was placed on a rotating drum and the latency(s) of each subject to fall from the rod was measured. Mice were given one training trial and two experimental trials for 2 days.

Foot-printing and stride length analysis: the soles of the fore and the hind paws were dyed in red and blue ink, respectively, and the mice were allowed to walk down an 80-cm runway lined with white paper. The stride lengths were analyzed by measuring the length of three consecutive strides.

### Determination of striatal dopamine and dopamine metabolite levels

To determine striatal dopamine and metabolites levels, animals were killed by cervical dislocation, brains were removed and the striata were dissected out on ice. The samples were immediately frozen and stored at -80°C until use. The tissues were processed for the analysis by high-performance liquid chromatography (HPLC) with electrochemical detector (ECD). The dissected tissues were weighed, homogenized and deproteinized in 0.2 N perchloric acid solution containing 7.9 mM Na<sub>2</sub>S<sub>2</sub>O<sub>5</sub> and 1.3 mM Na<sub>2</sub>EDTA. The homogenate was centrifuged at 37000 × *g* for

30 min and the supernatant was stored at -80°C until assayed. A reverse-phase ion-pair chromatography was used in all analyses and the mobile phase consisted of an acetonitrile-50 mM phosphate buffer pH 3.0, containing 5-octylsulfate sodium salt (300 mg/l) as the ion-pair reagent and (20 mg/l) Na<sub>2</sub>EDTA. Reference standards were prepared in 0.2 N perchloric acid solution containing 7.9 mM Na<sub>2</sub>S<sub>2</sub>O<sub>5</sub> and 1.3 mM Na<sub>2</sub>EDTA. Samples were quantified by comparison of the areas under the peaks with those of reference standards using HPLC software (Chromatography Station for Windows™, Watrex International Inc., San Francisco, CA).

### Immunohistochemistry

Mice were anaesthetized deeply with CO<sub>2</sub> and perfused intracardially with ice-cold phosphate buffer (PBS; pH 7.2) and subsequently with 4% paraformaldehyde in 0.1 M PBS (PFA). Brains were quickly removed, postfixed in PFA overnight at 4°C, cryoprotected in 15% sucrose in 0.1 M PBS for 24 h and in 30% sucrose in 0.1 M PBS for 24 h at 4°C, frozen and stored at -80°C until sectioning. Free-floating cryostat-cut sections (30 μ) were collected using a Bright cryostat at -20°C at the levels of striatum (AP, 0.2 mm from bregma) and the entire midbrain (AP, -5.6 mm from bregma) (51). Sections first were quenched for 10 min in 3% H<sub>2</sub>O<sub>2</sub>/10% methanol (52). Then sections were preincubated with 10% goat serum for 1 h and incubated with a polyclonal anti-TH antibody (1:2000; Calbiochem, San Diego, CA) or anti-ASYN syn-1 antibody (1:1000; BD Biosciences), or anti-CD45 (1:500, Abcam) for 48 h in 4°C, followed by incubation with biotinylated antirabbit antibody (1:1500; Vector Laboratories, Burlingame, CA) in 1% goat serum for 1 h and avidin-biotin peroxidase complex for 1 h in RT (ABC Elite; Vector Laboratories). Staining was visualized using DAB (Sigma; St. Louis, MO) as a chromogen. The specificity was tested in adjacent sections with the primary or the secondary antibody omitted. Sections were stained with cresyl violet (Nissl staining) as described previously (52) and then dehydrated in graded ethanol baths and coverslipped.

### Immunofluorescence

Mice were anesthetized and transcardially perfused as described above and stored at -80°C until sectioning. Serial coronal sections were cut at 35 μm using a microtome. The sections were washed 3 times with PBS-Triton 0.2%, blocked using 5% NGS in saline with 0.2% Triton and then incubated with anti-*Nurr1* Ab (1:100 dilution, Santa Cruz) or anti-Iba1 antibody (1:750 dilution, Wako Chemicals USA, Inc.) or antigalectin-3 (AF1197, 1:40 dilution, R&D Systems, Abingdon, United Kingdom) in PBS-Triton 0.2% overnight at 4°C. After three washes with PBS-Triton 0.3%, the sections were incubated with appropriate secondary fluorescent-labeled antibodies (1:1000, Molecular probes) in NGS 2% in PBS-Triton 0.2% for 1 h (RT). Cell nuclei were stained with DAPI or Hoechst 33382 and the sections were mounted using IMM mounting medium. Representative images were captured using an inverted fluorescence microscope equipped with a digital color camera. The signal of *Nurr1*-positive cells was quantitated as mean intensity/cell using ImageJ.

### Cell counting

The total number of SN TH-positive neurons were counted in both hemibrainstems by using the optical fractionator, an unbiased method of cell counting that is not affected by either the volume of reference or the size of the counted neurons. The

SN was delineated by using a computer-assisted image analysis system (52). TH-stained neurons were counted in every fourth section throughout the entire extent of the SN. As an anatomical reference, the standard mouse atlas was used (51).

Nissl-positive cell counts were the average of four different regions of corresponding sections for each genotype.

### Western blot analysis

Brain regions of cortex and spinal cord were rapidly dissected and lysed on ice in whole-cell lysis buffer (10 mL/1 g tissue) (150 mM NaCl, 50 mM Tris pH 7.6, 0.1% SDS, 1% Triton, 2 mM EDTA and protease inhibitors) and spun for 40 min at 50 000 × g at 4°C. The supernatant was kept at –80°C until use as Triton fraction. The pellet was resuspended in 1 M sucrose in STET buffer (150 mM NaCl, 50 mM Tris pH 7.6, 0.1% SDS, 2 mM EDTA) and spun for 30 min at 50 000 × g at 4°C. The myelin containing supernatant was removed and the pellet was resuspended in 2% SDS, 50 mM Tris pH 7.6. The samples after sonication and boiling were kept at –80°C until use as SDS fraction. Protein concentration was determined for each sample by the Bradford assay (Bio-Rad). Samples (20 µg of total protein) were separated on 10% polyacrylamide gel and then transferred to nitrocellulose. After 1 h of blocking in 5% non-fat dried milk at RT, the nitrocellulose was incubated overnight at 4°C with ASYN (BD, monoclonal Syn-1 Ab) 1:1000, or Nurr1 (N-20, Santa-Cruz) 1:500. The blot was rinsed with TBS-Tween and then incubated with horseradish peroxidase-conjugated antirabbit or antimouse (Pierce) antibody for 1 h at RT. Following further washes, blots were visualized with Western Lightning (PerkinElmer, Norwalk, CT, USA) and exposed to Super RX film (Fuji Film). Blots were stripped and reprobed with β-actin mouse monoclonal antibody (1:20 000; T5168; Sigma) or ERK rabbit polyclonal antibody (1:50 000, Santa Cruse Biotechnology) to verify equivalent protein loading.

### L-DOPA injections

L-DOPA (5 mg/kg) and carbidopa (0.5 mg/kg) were injected IP in experimental animals. Stride length measurements were done on four consecutive days in order to minimize the required handling and to give time for the mice to recover from the injections. Day 1: Measurement of the baseline stride length that is indicated with 1st bar in Fig. 4B. Day 2: Measurement of stride length in response to L-DOPA administration (2nd bar in Fig. 4B). Day 3: Because the condition of phenotypic mice frequently deteriorated by the day, we measured the baseline stride length again (3rd bar in Fig. 4B). Day 4: Measurement of stride length in response to saline administration (4th bar in Fig. 4B). The Day 1 baseline and the Day 2 response to L-DOPA were used in the calculations.

### Statistics

GraphPad Prism4 software was used for statistical analysis. Significance was assessed with the one- or two-way ANOVA test followed by post hoc Bonferroni's Multiple Comparison Test unless otherwise indicated. A P-value less than 0.05 was considered significant. Error bars represent ±SEM.

### Supplementary Material

Supplementary Material is available at HMG online.

### Acknowledgments

We would like to thank Dr Stelios Psarras and Dr Oeystein Roed Brekk for help with neuroinflammation experiments, and Dr Yannis Bassiakos for advice on statistical analyses. We thank Dr Benoit Giasson for helpful discussions and Dr Tomas Perlmann for providing the Nurr1+/- mice. We would also like to thank Dr Nikos Kostomitsopoulos, Director of the Animal Care Facilities, for facilitating our work.

**Conflict of Interest statement.** The authors declare no competing financial interests.

### Funding

Michael J Fox Foundation (to D.K.V. and L.S.); a University of Athens grant from the Hellenic Ministry of Health 'Thalis' (# 398 70/3/11679 to L.S. and D.K.V.); and by FP7/REGPOT-2008-1 (to L.S. and D.K.V.); M.A. was supported by a Hellenic General Secretariat of Research and Technology 'PENED' (#650 to D.K.V.).

### References

1. Driver, J.A., Logroscino, G., Gaziano, J.M. and Kurth, T. (2009) Incidence and remaining lifetime risk of Parkinson disease in advanced age. *Neurology*, **72**, 432–438.
2. Collier, T.J., Kanaan, N.M. and Kordower, J.H. (2011) Ageing as a primary risk factor for Parkinson's disease: evidence from studies of non-human primates. *Nat. Rev. Neurosci.*, **12**, 359–366.
3. Rodriguez, M., Rodriguez-Sabate, C., Morales, I., Sanchez, A. and Sabate, M. (2015) Parkinson's disease as a result of aging. *Aging Cell*, **4**, 293–308.
4. Spillantini, M.G., Schmidt, M.L., Lee, V.M.-Y., Trojanowski, J.Q., Jakes, R. and Goedert, M. (1997) α-Synuclein in Lewy bodies. *Nature*, **388**, 839–840.
5. Polymeropoulos, M.H., Lavedan, C., Leroy, E., Die, S.E., Dehejia, A., Dutra, A., Pike, B., Root, H., Rubenstein, J., Boyer, R. et al. (1997) Mutation in the alpha-synuclein gene identified in families with Parkinson's disease. *Science*, **276**, 2045–2047.
6. Singleton, A.B., Farrer, M., Johnson, J., Singleton, A., Hague, S., Kachergus, J., Hulihan, M., Peuralinna, T., Dutra, A., Nussbaum, R. et al. (2003) Alpha-Synuclein locus triplication causes Parkinson's disease. *Science*, **302**, 841.
7. Chartier-Harlin, M.C., Kachergus, J., Roumier, C., Mouroux, V., Douay, X., Lincoln, S., Leveque, C., Larvor, L., Andrieux, J., Hulihan, M. et al. (2004) Alpha-synuclein locus duplication as a cause of familial Parkinson's disease. *Lancet*, **364**, 1167–1169.
8. Breger, L.S. and Fuzzati Armentero, M.T. (2019) Genetically engineered animal models of Parkinson's disease: from worm to rodent. *Eur. J. Neurosci.*, **49**, 533–560.
9. Le, W.D., Xu, P., Jankovic, J., Jiang, H., Appel, S.H., Smith, R.G. and Vassilatis, D.K. (2003) Mutations in NR4A2 associated with familial Parkinson disease. *Nat. Genet.*, **33**, 85–89.
10. Hering, R., Petrovic, S., Mietz, E.M., Holzmann, C., Berg, D., Bauer, P., Weitalla, D., Müller, T., Berger, K., Krüger, R. and Riess, O. (2004) Extended mutation analysis and association studies of Nurr1 (NR4A2) in Parkinson disease. *Neurology*, **62**, 1231–1232.
11. Healy, D.G., Abou-Sleiman, P.M., Ahmadi, K.R., Gandhi, S., Muqit, M.M., Bhatia, K.P., Quinn, N.P., Lees, A.J., Holton, J.L.,

- Revesz, T. and Wood, N.W. (2006) NR4A2 genetic variation in sporadic Parkinson's disease: a genome-wide approach. *Mov. Disord.*, **21**, 1960–1963.
12. Grimes, D.A., Han, F., Panisset, M., Racacho, L., Xiao, F., Zou, R., Westaff, K. and Bulman, D.E. (2006) Translated mutation in the Nurr1 gene as a cause for Parkinson's disease. *Mov. Disord.*, **21**, 906–909.
  13. Sleiman, P.M., Healy, D.G., Muqit, M.M., Yang, Y.X., Van Der Brug, M., Holton, J.L., Revesz, T., Quinn, N.P., Bhatia, K., Diss, J.K. et al. (2009) Characterisation of a novel NR4A2 mutation in Parkinson's disease brain. *Neurosci. Lett.*, **457**, 75–79.
  14. Zetterström, R.H., Solomin, L., Jansson, L., Hoffer, B.J., Olson, L. and Perlmann, T. (1997) Dopamine neuron agenesis in Nurr1-deficient mice. *Science*, **276**, 248–250.
  15. Saucedo-Cardenas, O., Quintana-Hau, J.D., Le, W.D., Smidt, M.P., Cox, J.J., De Mayo, F., Burbach, J.P. and Conneely, O.M. (1998) Nurr1 is essential for the induction of the dopaminergic phenotype and the survival of ventral mesencephalic late dopaminergic precursor neurons. *Proc. Natl. Acad. Sci. USA.*, **95**, 4013–4018.
  16. Zhang, L., Le, W., Xie, W. and Dani, J.A. (2012) Age-related changes in dopamine signaling in Nurr1 deficient mice as a model of Parkinson's disease. *Neurobiol. Aging*, **33**, 7–16.
  17. Le, W.D., Conneely, O.M., He, Y., Jankovic, J. and Appel, S.H. (1999) Reduced Nurr1 expression increases the vulnerability of mesencephalic dopamine neurons to MPTP-induced injury. *J. Neurochem.*, **73**, 2218–2221.
  18. Saijo, K., Winner, B., Carson, C.T., Collier, J.G., Boyer, L., Rosenfeld, M.G., Gage, F.H. and Glass, C.K. (2009) A Nurr1/CoREST pathway in microglia and astrocytes protects dopaminergic neurons from inflammation-induced death. *Cell*, **137**, 47–59.
  19. Chu, Y. and Kordower, J.H. (2007) Age-associated increases of alpha-synuclein in monkeys and humans are associated with nigrostriatal dopamine depletion: is this the target for Parkinson's disease? *Neurobiol. Dis.*, **25**, 134–149.
  20. Kazantsev, A.G. and Kolchinsky, A.M. (2008) Central role of alpha-synuclein oligomers in neurodegeneration in Parkinson disease. *Arch. Neurol.*, **65**, 1577–1581.
  21. Chu, Y., Kompoliti, K., Cochran, E.J., Mufson, E.J. and Kordower, J.H. (2002) Age-related decreases in Nurr1 immunoreactivity in the human substantia nigra. *J. Comp. Neurol.*, **450**, 203–214.
  22. Chu, Y., Le, W., Kompoliti, K., Jankovic, J., Mufson, E.J. and Kordower, J.H. (2006) Nurr1 in Parkinson's disease and related disorders. *J. Comp. Neurol.*, **494**, 495–514.
  23. Baptista, M.J., O'Farrell, C., Daya, S., Ahmad, R., Miller, D.W., Hardy, J., Farrer, M.J. and Cookson, M.R. (2003) Co-ordinate transcriptional regulation of dopamine synthesis genes by alpha-synuclein in human neuroblastoma cell lines. *J. Neurochem.*, **85**, 957–968.
  24. Lin, X., Parisiadou, L., Sgobio, C., Liu, G., Yu, J., Sun, L., Shim, H., Gu, X.L., Luo, J., Long, C.X. et al. (2012) Conditional expression of Parkinson's disease-related mutant  $\alpha$ -synuclein in the midbrain dopaminergic neurons causes progressive neurodegeneration and degradation of transcription factor nuclear receptor related 1. *J. Neurosci.*, **32**, 9248–9264.
  25. Decressac, M., Kadkhodaei, B., Mattsson, B., Laguna, A., Perlmann, T. and Björklund, A. (2012)  $\alpha$ -Synuclein-induced down-regulation of Nurr1 disrupts GDNF signaling in nigral dopamine neurons. *Sci. Transl. Med.*, **4**, 163ra156.
  26. Bobela, W., Aebischer, P. and Schneider, B.L. (2015) Alpha-Synuclein as a mediator in the interplay between aging and Parkinson's disease. *Biomol. Ther.*, **5**, 2675–2700.
  27. Oita, R.C., Mazzatti, D.J., Lim, F.L., Powell, J.R. and Merry, B.J. (2009) Whole-genome microarray analysis identifies up-regulation of Nr4a nuclear receptors in muscle and liver from diet-restricted rats. *Mech. Ageing Dev.*, **130**, 240–247.
  28. Giasson, B.I., Duda, J.E., Quinn, S.M., Zhang, B., Trojanowski, J.Q. and Lee, V.M. (2002) Neuronal alpha-synucleinopathy with severe movement disorder in mice expressing A53T human alpha-synuclein. *Neuron*, **34**, 521–533.
  29. Bäckman, C., You, Z.B., Perlmann, T. and Hoffer, B.J. (2003) Elevated locomotor activity without altered striatal dopamine contents in Nurr1 heterozygous mice after acute exposure to methamphetamine. *Behav. Brain Res.*, **143**, 95–100.
  30. Rojas, P., Joodmardi, E., Hong, Y., Perlmann, T. and Ogren, S.O. (2007) Adult mice with reduced Nurr1 expression: an animal model for schizophrenia. *Mol. Psychiatry*, **12**, 756–766.
  31. Tofaris, G.K., Garcia Reitböck, P., Humby, T., Lambourne, S.L., O'Connell, M., Ghetti, B., Gossage, H., Emson, P.C., Wilkinson, L.S., Goedert, M. and Spillantini, M.G. (2006) Pathological changes in dopaminergic nerve cells of the substantia nigra and olfactory bulb in mice transgenic for truncated human alpha-synuclein(1-120): implications for Lewy body disorders. *J. Neurosci.*, **26**, 3942–3950.
  32. Daher, J.P., Ying, M., Banerjee, R., McDonald, R.S., Hahn, M.D., Yang, L., Flint Beal, M., Thomas, B., Dawson, V.L., Dawson, T.M. and Moore, D.J. (2009) Conditional transgenic mice expressing C-terminally truncated human alpha-synuclein (alphaSyn119) exhibit reduced striatal dopamine without loss of nigrostriatal pathway dopaminergic neurons. *Mol. Neurodegeneration*, **24**, 34.
  33. Tsika, E., Moysidou, M., Guo, J., Cushman, M., Gannon, P., Sandaltzopoulos, R., Giasson, B.I., Krainc, D., Ischiropoulos, H. and Mazzulli, J.R. (2010) Distinct region-specific alpha-synuclein oligomers in A53T transgenic mice: implications for neurodegeneration. *J. Neurosci.*, **30**, 3409–3418.
  34. Kurz, A., Double, K.L., Lastres-Becker, I., Tozzi, A., Tantucci, M., Bockhart, V., Bonin, M., García-Arencibia, M., Nuber, S., Schlaudraff, F. et al. (2010) A53T-alpha-synuclein overexpression impairs dopamine signaling and striatal synaptic plasticity in old mice. *PLoS One*, **5**, e11464.
  35. Boza-Serrano, A., Reyes, J.F., Rey, N.L., Leffler, H., Bousset, L., Nilsson, U., Brundin, P., Venero, J.L., Burguillos, M.A. and Deierborg, T. (2014) The role of Galectin-3 in  $\alpha$ -synuclein-induced microglial activation. *Acta Neuropathol. Commun.*, **2**, 156.
  36. Siew, J.J., Chen, H.M., Chen, H.Y., Chen, H.L., Chen, C.M., Soong, B.W., Wu, Y.R., Chang, C.P., Chan, Y.C., Lin, C.H., Liu, F.T. and Chern, Y. (2019) Galectin-3 is required for the microglia-mediated brain inflammation in a model of Huntington's disease. *Nat. Commun.*, **10**, 3473.
  37. Sotiriou, E., Vassilatis, D.K., Vila, M. and Stefanis, L. (2010) Selective noradrenergic vulnerability in  $\alpha$ -synuclein transgenic mice. *Neurobiol. Aging*, **31**, 2103–2114.
  38. Niccoli, T. and Partridge, L. (2012) Ageing as a risk factor for disease. *Curr. Biol.*, **22**, R741–R752.
  39. Johnson, I.P. (2015) Age-related neurodegenerative disease research needs aging models. *Front. Aging Neurosci.*, **7**, 168.
  40. Kim, K.S., Kim, C.H., Hwang, D.Y., Seo, H., Chung, S., Hong, S.J., Lim, J.K., Anderson, T. and Isacson, O. (2003) Orphan nuclear receptor Nurr1 directly transactivates the promoter activity of the tyrosine hydroxylase gene in a cell-specific manner. *J. Neurochem.*, **85**, 622–634.
  41. Spathis, A.D., Asvos, X., Ziavra, D., Karampelas, T., Topouzis, S., Cournia, Z., Qing, X., Alexakos, P., Smits, L.M., Dalla, C. et

- al. (2017) Nurr1:RXR $\alpha$  heterodimer activation as monotherapy for Parkinson's disease. *Proc. Natl. Acad. Sci. USA.*, **114**, 3999–4004.
42. Kojovic, M., Kassavetis, P., Bologna, M., Pareés, I., Rubio-Agusti, I. and Bhatia, K.P. (2015) Transcranial magnetic stimulation follow-up study in early Parkinson's disease: a decline in compensation with disease progression? *Mov. Disord.*, **30**, 1098–1106.
  43. Sundström, E., Strömberg, I., Tsutsumi, T., Olson, L. and Jonsson, G. (1987) Studies on the effect of 1-methyl-4-phenyl-1,2,3,6-tetrahydropyridine (MPTP) on central catecholamine neurons in C57BL/6J mice. Comparison with three other strains of mice. *Brain Res.*, **405**, 26–38.
  44. Muthane, U., Ramsay, K.A., Jiang, H., Jackson-Lewis, V., Donaldson, D., Fernando, S., Ferreira, M. and Przedborski, S. (1994) Differences in nigral neuron number and sensitivity to 1-methyl-4-phenyl-1,2,3,6-tetrahydropyridine in C57/bl and CD-1 mice. *Exp. Neurol.*, **126**, 195–204.
  45. Sedelis, M., Hofele, K., Auburger, G.W., Morgan, S., Huston, J.P. and Schwarting, R.K. (2000) MPTP susceptibility in the mouse: behavioral, neurochemical, and histological analysis of gender and strain differences. *Behav. Genet.*, **30**, 171–182.
  46. Mak, S.K., McCormack, A.L., Langston, J.W., Kordower, J.H. and Di Monte, D.A. (2009) Decreased alpha-synuclein expression in the aging mouse substantia nigra. *Exp. Neurol.*, **220**, 359–365.
  47. Kim, C., Ho, D.H., Suk, J.E., You, S., Michael, S., Kang, J., Joong Lee, S., Masliah, E., Hwang, D., Lee, H.J. and Lee, S.J. (2013) Neuron-released oligomeric  $\alpha$ -synuclein is an endogenous agonist of TLR2 for paracrine activation of microglia. *Nat. Commun.*, **4**, 1562.
  48. Yang, Y.X. and Latchman, D.S. (2008) Nurr1 transcriptionally regulates the expression of alpha-synuclein. *Neuroreport*, **19**, 867–871.
  49. Jia, C., Qi, H., Cheng, C., Wu, X., Yang, Z., Cai, H., Chen, S. and Le, W. (2020) Alpha-Synuclein negatively regulates Nurr1 expression through NF-kB-related mechanism. *Front. Mol. Neurosci.*, **13**, 64.
  50. Kim, C.H., Han, B.S., Moon, J., Kim, D.J., Shin, J., Rajan, S., Nguyen, Q.T., Sohn, M., Kim, W.G., Han, M. et al. (2015) Nuclear receptor Nurr1 agonists enhance its dual functions and improve behavioral deficits in an animal model of Parkinson's disease. *Proc. Natl. Acad. Sci. USA.*, **112**, 8756–8761.
  51. Paxinos, G. and Franklin, K.B.J. (2001) *The Mouse Brain in Stereotaxic Coordinates*. 2. Academic Press, San Diego.
  52. Jackson-Lewis, V., Vila, M., Djaldetti, R., Guegan, C., Liberatore, G., Liu, J., O'Malley, K.L., Burke, R.E. and Przedborski, S. (2000) Developmental cell death in dopaminergic neurons of the substantia nigra of mice. *J. Comp. Neurol.*, **424**, 476–488.